Nano-Mechanical Properties and Topography of Thermosetting Acrylic Powder Coatings

D.C. Andrei, J.L. Keddie†, and J.N. Hay—University of Surrey*
S.G. Yeates—Avecia Ltd.**
B.J. Briscoe and D. Parsonage—Imperial College††

Both nano-scratching and nano-indentation techniques have been used to evaluate the mechanical properties of the surface of acrylic coatings, with and without added pigment. The coatings were formed from thermosetting, acrylic powders. Both types of coatings—clear and pigmented—do not exhibit any significant differences in their hardness with an increase in baking time from 7 to 15 min. According to the scratching profiles, the deformation induced at the surface is virtually elastic. Introducing the pigment causes a slight increase in the elastic modulus but no significant variation in hardness. In all coatings, the computed hardness and the elastic modulus values are higher near the surface (perhaps as a result of tip geometry effects), but these readily reach plateau values that are consistent with other work available in the literature. A long-range surface profiler, which provided two-dimensional and three-dimensional topographical maps of the coating surfaces, reveals undulations in the surface with a wavelength on the order of 2-4 mm. Moreover, the topography of the pigmented coating is significantly smoother than that of the clear coating in which shallow pits (about 100 μm in diameter) are randomly distributed at the surface. The nano-mechanical properties within these pits are similar to the bulk of the coating.

INTRODUCTION

The production of powder coatings has undergone a substantial increase in recent years worldwide, with Europe being the leader for their usage.[1] The use of powders provides unique advantages such as the non-emission of solvents, significant energy savings, excellent adhesion to many substrates, and the production of a good finish. Although the coatings are generally fairly smooth, the classical "orange peel" appearance is still present in many cases. Also, additional defects may be present[2,3] such as pinholes, impurities, etc. It is also unclear if the surface topography of powder coatings correlates with their mechanical properties.

The recent development of nano-techniques has allowed a more accurate analysis of the intrinsic mechanical properties of the surfaces of such coatings. Among the various types of investigation, scratching techniques have proved especially useful in evaluating the potential of a particular coating to avoid the development of relatively fine, visually apparent scratches that spoil the coating's appearance, which is usually termed "mar resistance." Moreover, the scratching techniques, along with more conventional indentation procedures (often performed with the same equipment), provide useful information about deformation in the coatings (i.e., whether elastic, plastic or viscoelastic), as well as their roughness and mechanical constants (e.g., their hardness and elastic modulus).

As early as 1952, Schallamach[4] used scratching techniques to evaluate the mechanisms of friction and abrasion of elastomeric materials, albeit on a macroscopic scale. Even now, this work is a valuable reference on the response of soft and highly elastic surfaces to scratching. More recently, the scratch hardness of glassy, thermoplastic polymers under a number of contact conditions was studied by Briscoe et al.[5] The same group used the compliance method and a calibration technique to ac-

*Author to whom correspondence should be addressed.
†School of Physics and Chemistry, Guildford, Surrey, GU2 7XH, UK. (keddie@surrey.ac.uk, j.hay@surrey.ac.uk)
**Hexagon House, P.O. Box 42, Blackley, Manchester M9 8ZS, UK. (stephen.yeates@avecia.com)
††Department of Chemical Engineering and Chemical Technology, Prince Consort Road, London SW7 2BY (b.briscoe@ic.ac.uk)

Table 1—Characteristics of the Epoxy Functional Acrylic Terpolymer (GMA1)

Epoxy equivalent weight	396
M_w (PS equivalent)	5720
M_n (PS equivalent)	3290
Polydispersity	1.7
Midpoint T_g (°C)	42
ICI C/P Viscosity @ 165°C (Poise)	90

count for the tip geometry in a study of several glassy thermoplastic surfaces.[6] Scratch hardness measurements were also used to investigate the effects of plasticization by solvents upon the mechanical properties of glassy polymer surfaces.[7]

For many decades, indentation techniques have been used to determine the hardness of coatings.[8] Recent work has shown that the conical styluses, sometimes used for both indentation and scratching, may provide a useful means of differentiating between different types of deformation processes (i.e., elastic, plastic, and elastic-plastic)[9] induced in the systems. Although values for the hardness of the coating, as well as estimates of the adhesion to the substrate, may be obtained, the conical stylus method shows limitations in assessing the appearance of very discrete scratches on the coating. AFM may successfully be used for such a purpose.[10] In one of the first studies of its kind, Courter[11] applied the stylus method to clear, crosslinked acrylic coatings. Values for the Young's modulus as a function of depth of penetration were obtained. The work also presented scratching maps over relatively large distances (3 mm) and low penetration depths (ca. 20 µm). The same author also provided an interesting correlation between the coating mechanical properties and the corresponding "mar resistance."[12] Related investigations of the mar behavior of polymer surfaces using micro- and nano-wear testing have also been reported.[13,14] There has been very little else published, however, on the use of nano-mechanical techniques to characterize the surfaces of organic coatings, and the effects of included pigment have been largely unexplored.

In the present study, nano-instruments were used for studying both clear and pigmented crosslinked, acrylic coatings. Until now, there has been no systematic study that has aimed to determine the effects of pigment, if any, on the mechanical properties of such coating surfaces. Moreover, this work aims to determine if variations in surface topography lead to systematic variations in nano-mechanical properties.

The current study additionally provides information about the proportion of elastic, viscous, and fracture deformation during the nano-scratching of the coatings. It is well known that for low applied forces, upon removal of the load, there will be no apparent permanent damage or deformation to the coating. If the normal force is increased or a sharper indenter is used in the process, then the coating will yield or fracture according to its intrinsic mechanical characteristics. If the extent of the contact deformation exceeds the yielding potential, the material undergoes some permanent deformation (e.g., a "valley" with "hills" along the sides is produced) or fractures are generated (in the case of severe environments). In this work, the scratches showed essentially a complete geometric recovery of the crosslinked acrylic surfaces under investigation, indicative of an elastic (not plastic) behavior, which is characteristic of elastomeric coatings.

EXPERIMENTAL

Materials

Work reported here used an experimental solid epoxy functional acrylic terpolymer (referred to as GMA1) supplied by Avecia Ltd. The GMA1 terpolymer was synthesized from methyl methacrylate, butyl methacrylate, and glycidyl methacrylate. The physical properties of the GMA1 resin are given in *Table* 1.

The GMA1 resin was the binder in both a standard clearcoat formulation (Formulation A) and a standard high gloss white formulation using titanium dioxide pigment TiO_2 2160, from Kronos, (Formulation B). In both formulations, a multifunctional carboxylic acid hardener based upon hexane diisocyanate, Crelan VP LS 2125, from Bayer, (with an acid value of 465 mg KOH/g and a functionality of 2.3) functioned as the crosslinker and was used in a GMA1:crosslinker weight ratio of 2.84:1. The formulations contained benzoin as an anti-pinhole agent. *Table* 2 gives full details of the formulations.

Formulations were extruded at 200 rpm and 70 torque via a Gay's twin screw extruder with a barrel temperature profile of 50/110°C. The milled and classified (70 µm mesh) extrudate was applied onto 0.9 mm phosphated bonderite steel using a PG1 spray gun (Gema, Volstatic Industry Powder Systems, Switzerland).

The average particle size and shape can be seen in *Figures* 1 and 2, which show representative scanning electron microscope (SEM) images of the clear and pigmented powder coatings, respectively. (Experimental details about the SEM analysis are provided in the next section.) Both types of powder have a rather broad particle size distribution with particles being irregular in shape and highly faceted. There are no major differences in appearance between the two formulations.

Table 2—Formulations of the Clear and Pigmented Powders

Component	Formulation A Clearcoat (wt%)	Formulation B Pigmented Coating (wt%)
GMA1 resin	69.3	55.1
Carboxylic hardener[a]	24.4	19.4
Titanium dioxide pigment[b]	0	22.9
Benzoin	0.8	.2
Flow agent[c]	1.5	0.2
Dispersant[d]	1.2	1.2
Other additives[e]	2.8	0

(a) Crelan VP LS 2125, Bayer.
(b) TiO- 2160, Kronos.
(c) Modaflow III, Monsanto.
(d) Solsperse 26000, Avecia.
(e) 2:1 weight ratio of Tinuvin 900 :Tinuvin 144 , Ciba-Geigy.

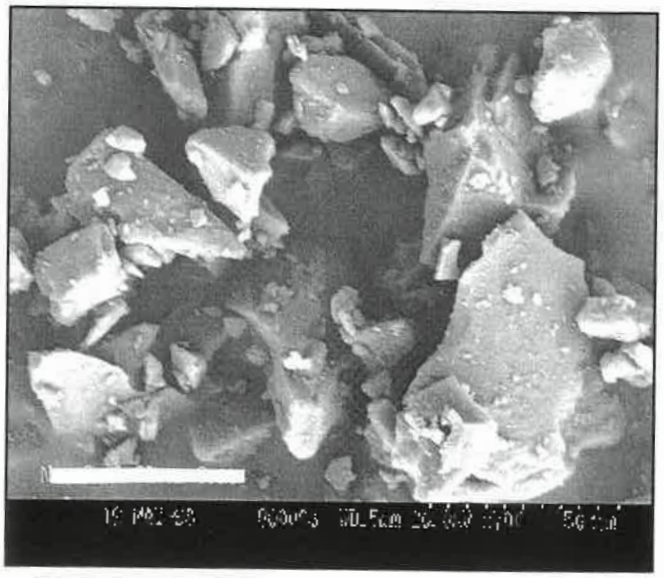

Figure 1—SEM micrograph of Formulation A (clearcoat) powders in their as-received state. A wide distribution in size is apparent. The shape of the particles is irregular with sharp edges. The bar indicates 50 µm.

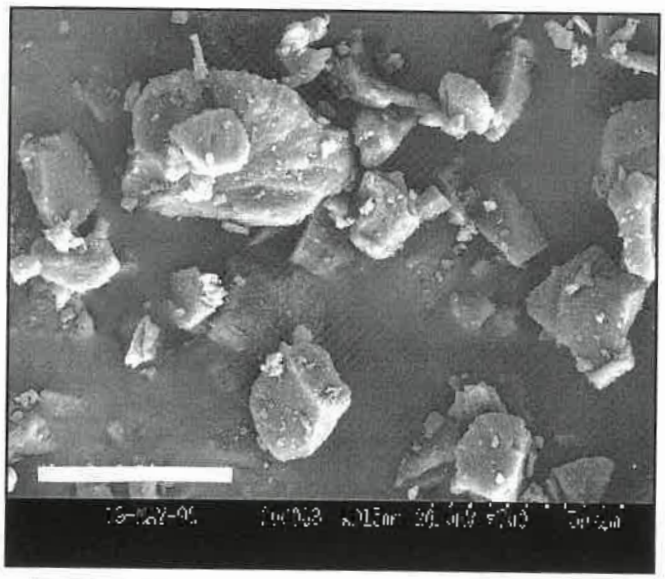

Figure 2—SEM micrograph of Formulation B (TiO_2-pigmented) powders in their as-received state. On average, there are no noticeable differences in the size and shape of the particles in comparison to the clearcoat shown in Figure 1. The bar indicates 50 µm.

The substrates with the deposited powder were introduced into a preheated oven at 150°C for the various baking times of 7, 11, and 15 min. (Note that 15 min is the standard, recommended baking time for Formulations A and B.) After curing, the coating thicknesses were in the range of 120-180 µm for the clearcoats and 50-70 µm for the pigmented samples. Spraying conditions of the powders were the same for both types of sample. The difference in final thickness values is attributed to differing charge transfer efficiencies of the two formulations.

Thermal Analysis

Modulated temperature differential scanning calorimetry (MTDSC) was used to determine the extent of crosslinking that occurs in the acrylic powders below the baking temperature. MTDSC is a relatively new calorimetric technique[15,16] that relies on the basic principles of conventional DSC but with the major difference being that it uses a heating ramp containing a sinusoidal perturbation. In recent years, it has been used successfully for the investigation of structural phase transitions,[17] thermal characterization of multicomponent systems,[18] separation of thermal processes with different kinetics or mechanisms,[19,20] and more accurate measurement of heat capacity.[21] This additional information may provide further insight into the structure and behavior of materials. In the case of powder coatings, conventional DSC is routinely used for measuring the characteristics of the thermal transitions.[22,23] Very little work has been published on MTDSC performed on thermosetting systems[24] in general and with even less on thermosetting powders. MTDSC analysis is superior to conventional DSC in the case of thermosetting acrylic powders, because it can de-convolute the peaks corresponding to the glass transition of the polymer, the melting of the crosslinker, and the crosslinking of the polymer, thereby allowing a more accurate determination of these temperatures. Typically, the crosslinker "melt" endotherm and acrylic "cure" exotherm occur simultaneously and would not be easily interpretable with a standard DSC experiment. With MTDSC, however, the melt and cure stages are readily resolved in the reversing and non-reversing signals. The pigmented and non-pigmented powders were both analyzed using a 2920 TA Instruments (Leatherhead, UK) calorimeter with a heating rate of 1°C/min.

Chemorheological Analysis

The flow properties of the powders (both Formulations A and B) were recorded on a Rheometrics RDSII dynamic rheometer. The instrument was operated at 10% strain using a parallel plate geometry with a 2 mm gap and a frequency of 10 rad.s^{-1}. Strain sweep measurements showed no evidence for non-linearity under these conditions. The temperature ramp rate was 10°C/min for all experiments.

Topographical Analysis

The surface topography of the coatings' surfaces was obtained with a three-dimensional contact profilometer (Dektak V200-Se). Areas as large as 1 cm × 1 cm were analyzed. Additional information was gained from scanning electron microscopy with an Hitachi S3200N instrument, typically with an accelerating voltage of 20 kV. The samples were coated with a thin layer of gold prior to analysis.

Scratching Experiments

The same instrument was used for performing both the scratching and the indentation experiments (Nanoindenter II, supplied by Nano-Instruments, Oak Ridge,

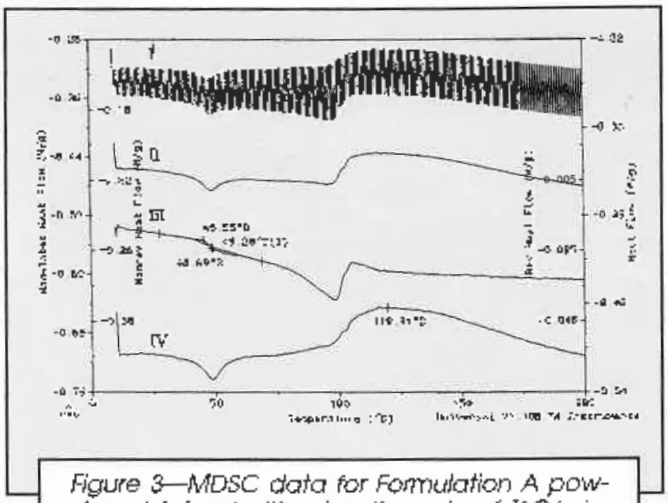

Figure 3—MDSC data for Formulation A powders obtained with a heating rate of 1°C/min. The curves are identified with a Roman numeral as follows: I is modulated heat flow (see left axis); II is total heat flow (right axis); III is reversing heat flow (right axis); and IV is non-reversing heat flow (left axis).

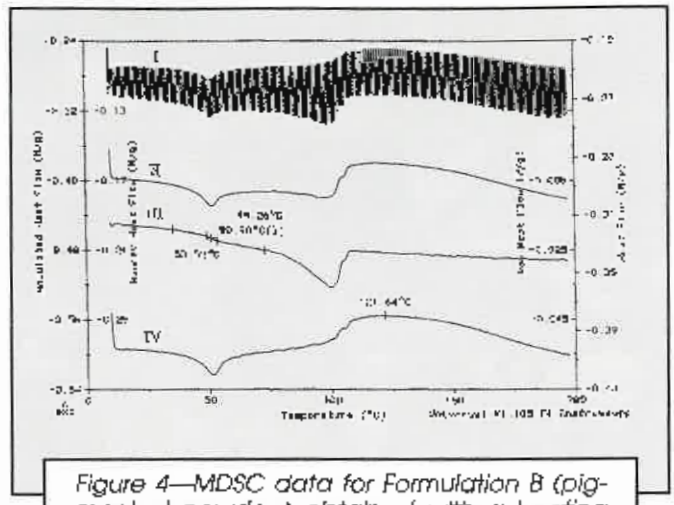

Figure 4—MDSC data for Formulation B (pigmented powders) obtained with a heating rate of 1°C/min. The curves are identified with a Roman numeral as follows: I is modulated heat flow (see left axis); II is total heat flow (right axis); III is reversing heat flow (right axis); and IV is non-reversing heat flow (left axis).

TN, USA). The instrument uses a compliance indentation system, capable of operating at loads in the microgram range and with a theoretical depth resolution on the sub-nanometer scale. It provides data on the Young's modulus and the hardness of the coatings. Unlike conventional hardness testers, the instrument does not require an optical measurement of the area of the indentation in order to calculate the hardness. The position of the indenter relative to the surface of the specimen is constantly monitored and hence, from a knowledge of the geometry of the tip, the area of the indentation is then calculated.

The Nano-Indenter II is essentially a load-controlled system, where the applied load is continuously monitored. The indenter tip is in the shape of a three-sided diamond pyramid, machined so that the sides make an angle of 65.3° with the normal to the base. The indentations appear as equilateral triangles, and the length of a side of an indentation is approximately 7.4 times its depth. The depth of an indentation, h, is equal to 0.113 times the diameter of the circle that circumscribes the indentation made on a surface. Attached to the top of the indenter rod, there is a coil held in a magnetic field. Thus, passage of a current through the coil can be used to apply a force to the indenter. The "zero point" contact for the present system was chosen where the machine stiffness becomes equal to 1.5 times its typical value. More details about the apparatus components are presented elsewhere.[25,26]

Scratches were made on the coating surface up to a depth of ca. 1.5 μm. This penetration depth, being less than one-tenth of the thickness of the coating, avoids the so-called "substrate effects." Since the theoretical depth resolution of the instrument is ± 0.04 nm, the indenter has the advantage of providing information about the very near surface of a specimen.

Each complete scratch procedure had five steps as follows. First, the surface is pre-scratched at a very low constant applied load of 20 μN over 500 μm with a constant velocity of 10 nm/sec. This first step provides a reference for the calculation of the scratch penetration depth. Then the stylus returns for a distance of 100 μm with the same velocity. Next, the scratch is performed deep in the coating with the same velocity of 10 nm/sec. After releasing the load, the stylus returns to the initial point. In the final step, the surface is profiled again as in the first step, in order to check for plastic deformation.

In addition, the nano-indenter can record the frictional drag force during scratching, which allows the calculation of the coefficient of friction between the stylus and sample surfaces. Two scratches of different depths were performed for each formulation.

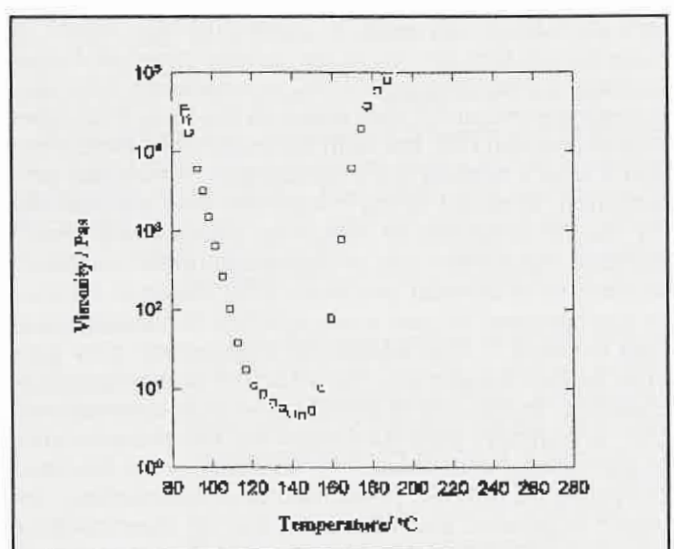

Figure 5—Chemo-rheological data for Formulation A (GMA1 crosslinked with Crelan LF21125). Viscosity (obtained as described in the text) decreases by about four orders of magnitude as temperature is increased.

Hardness and Young's Modulus Measurements

The hardness and Young's modulus were measured by performing an indentation experiment to a depth of ca. 700 nm deep into the surface. Each complete hardness test was performed via the following procedure. First, the stylus is lowered at a velocity of 10 nm/sec until the stiffness of the spring becomes 100 N/m, which is equal to 1.2 times the spring support stiffness of 84 N/m. At this point, the contact is considered to be reached. The load is increased at a rate of 5 μN/sec over a distance of 700 nm and then held for 60 sec. (The velocity of indentation was 5 nm/sec.) The load is then decreased at the initial rate to 80% of the final displacement, at which point the load is held for 60 sec. Finally, the load is released at 300 μN/sec.

Six indentations were performed on each sample surface, and these measurements were averaged. There is a slight variation in the range of indentation for the clear and pigmented coatings since the experiment is controlled by an upper limit of the permitted force on the cantilever. Any observable defects on the surface of the clear coatings were avoided and not included when finding the averages.

The continuous stiffness method was used for the evaluation of the Young's modulus and hardness. This method continuously measures the stiffness of contact between the indenter tip and the sample. During the loading procedure, an oscillatory mechanical force of known magnitude is applied to the mechanical contact junction between the indenter and the sample. An indication of the stiffness of contact between the tip and the sample is given by simultaneously measuring the phase shift between the force and the amplitude of the resulting oscillatory displacement between the tip and the sample. The Poisson's ratio (μ) was taken as 0.25 in the data analysis, which is a standard value[6,7] used for glassy polymer surfaces. In any case, the calculated values of nano-hardness and elastic modulus scale inversely with $(1 - \mu^2)$, and thus the calculated values are not particularly sensitive to the value of μ used.

RESULTS AND DISCUSSION

Thermal Analysis

MTDSC curves for the non-pigmented and pigmented acrylic powder (Formulations A and B) are presented in *Figures* 3 and 4, respectively. The reversing heat flow curves (which are given by the cyclic heat flow within the sample) show a glass transition for the non-pigmented acrylic at ca. 49°C. There is an increase in the value by only 1°C when the powder contains the pigment. These values of the glass transition temperature for the formulations are slightly higher than that obtained for the neat GMA1 resin (42°C as shown in *Table* 1). In both *Figures* 3 and 4, a melting peak of the crosslinking agent centered around 100°C may be identified. Also, the non-reversing heat flow curve (which is given by the subtraction from the total heat flow of the cyclic heat flow within the sample) shows a peak for the crosslinking (i.e., curing) process at around 120°C. These results reveal that the introduction of the pigment does not significantly influence the thermal constants of the acrylic and therefore the baking conditions.

Chemo-Rheology

From the determination of the viscosity/temperature profile of a thermoset powder coating it is possible to characterize both the flow and cure processes.[27] *Figure* 5 shows the result for clearcoat Formulation A, with analogous results being also obtained for pigmented Formulation B. The measured minimum viscosity is 2.7 Pa s. The onset temperature for rapid cure appears at about 150°C resulting in a limiting crosslink density as given by G' (i.e., the storage modulus at full cure, as defined by the plateau in the viscosity/temperature curve) of $>10^6$ Pa. Based on the MTDSC and these rheology measurements, it was determined that 150°C is adequate to use

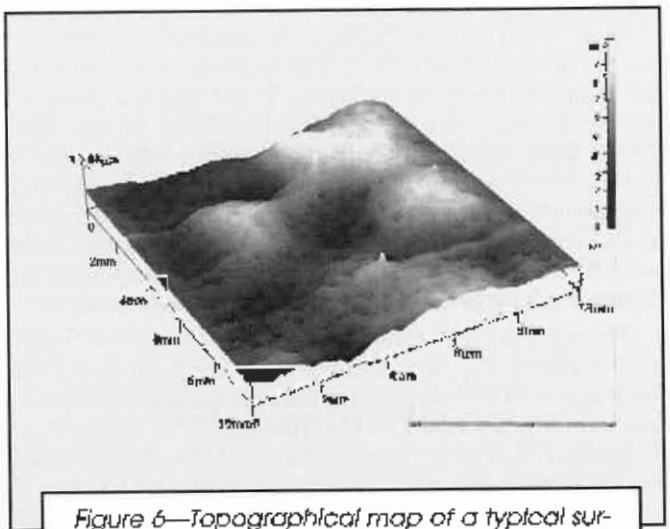

Figure 6—Topographical map of a typical surface of the clearcoat surface (Formulation A) over an area of 10 mm x 10 mm. Small dimples are seen distributed across the surface in addition to surface undulations.

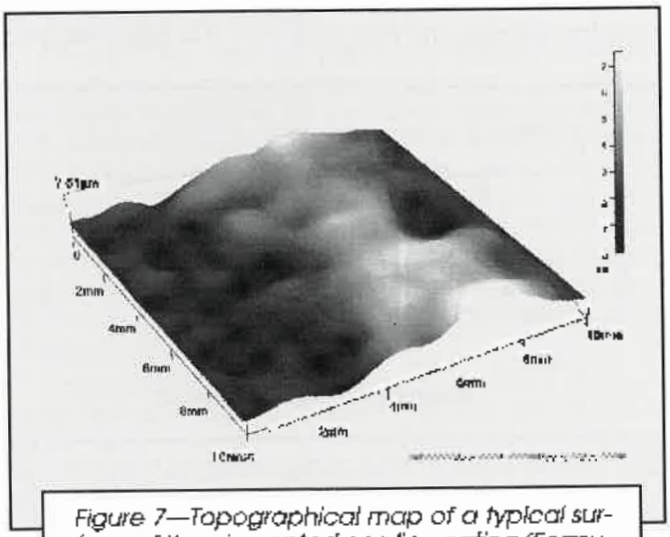

Figure 7—Topographical map of a typical surface of the pigmented acrylic coating (Formulation B) over an area of 10 mm x 10 mm.

as the reference cure temperature. Heating both formulations to this temperature apparently produced hard, glossy coatings for cure times of seven minutes or more.

Coating Topography

Visual inspection of the coatings reveals a marked unevenness in the surface finish that detracts from its appearance. The non-pigmented coatings also contain small defects, barely visible to the unaided eye, that are suggestive of the presence of "pinholes." *Figures* 6 and 7 show two typical topographies of clear and pigmented coatings, respectively. In both, there are variations in coatings thickness extending laterally over several mm. That is, undulations are apparent at the surface with a wavelength on the order of ca. 2-4 mm. The peak-to-valley height of the undulations are up to 20 µm. In the case of the clearcoating (*Figure* 6), dimples with an average diameter of about 100 µm are randomly distributed over the surface. A closer examination with SEM at a glancing angle has revealed that the dimples are very shallow, with no morphological differences in comparison to the rest of the film. It was also found by SEM that the dimples have oval shapes. These shallow dimples are presumed to be the defects visible to the eye and which were mistakenly considered to be pinholes. There is no evidence from the topography shown in *Figure* 7 (pigmented coating) that the pigment particles are present at the surface. Additionally, the morphology observed with SEM of this surface does not reveal any separate pigment phase at the surface but shows only binder.

The relationship between the formation of the "hills" and "valleys" (i.e., the "orange peel" configuration) and the inefficient flow following the application of the powder is often described in the literature.[2,20,25] It has been suggested that large agglomerates of powder particles resulting from the spray process lead, during baking, to undulations of the surface, as observed here. The length scale of the surface undulations (2-4 mm) are at least an order of magnitude greater than the particle powder size (20-100 µm), which is consistent with the concept of particle agglomerates as their source.

Other workers have observed "micro-pinholing" in powder coatings, and they attributed it to vapor trapped within the powder particles.[2] The micro-dimples found at the surface of the clearcoats are relatively shallow and therefore, although having a visual appearance of pinholes, are clearly not this type of defect. The fact that no morphological differences can be seen also suggests that these "defects" belong to the class of "orange peel" features.

The fact that these dimples are not present in the case of pigmented coatings might suggest a more uniform deposition of the powder on the substrate in the presence of pigment. Theories of surface flattening[28,29] predict that surface undulations in thicker coatings should level to a plane at a faster rate than thicker coatings. As the clearcoat is about twice as thick as the pigmented coating, it is surprising, therefore, that the thicker clearcoating is less flat. Theory[29] also predicts that small undulations—such as the micro-dimples—will flatten faster than larger waves at the surface. The origin of the dimples is therefore unlikely to be the poor levelling of pre-existing surface defects in the powder layer. Instead, lateral flow of the polymer melt during processing is being impeded or prevented. One explanation could be localized variations in viscosity or surface tension.

Nano-Scratching

Figures 8 and 9 show the responses to the various scratching cycles performed on the clear and pigmented acrylic coatings, respectively, both with baking times of 11 min. The pre-scratch profiles show that the surfaces are relatively smooth. Over distances of 15 µm, there is an average deviation of ± 40 nm from the central line, and the deviation is ±150 nm over lateral distances of 500 µm.

The actual scratches show a slight systematic difference in curvature between the clear and pigmented coats. The slightly more abrupt shape of the curve in the case of the pigmented coats suggests a somewhat harder coating. It should be noted that scratching is a continuous method of analysis and, hence, gives information about the coating as a continuum. Comparison of the results shown here with other measurements reveals that no significant differences between the samples with other baking times (7 and 15 min) for the same coating

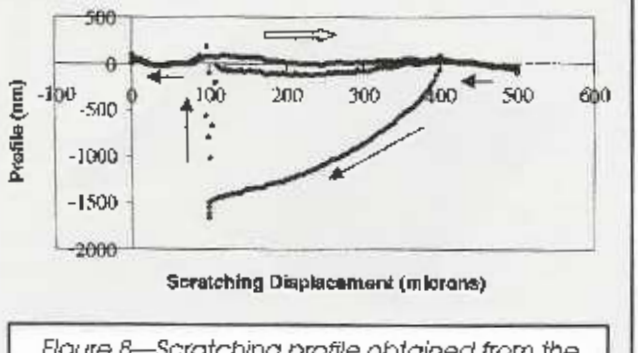

Figure 8—Scratching profile obtained from the surface of a clearcoat produced with 11 min of baking. Arrows show direction of the scratch. The thicker arrow indicates the route that was followed twice.

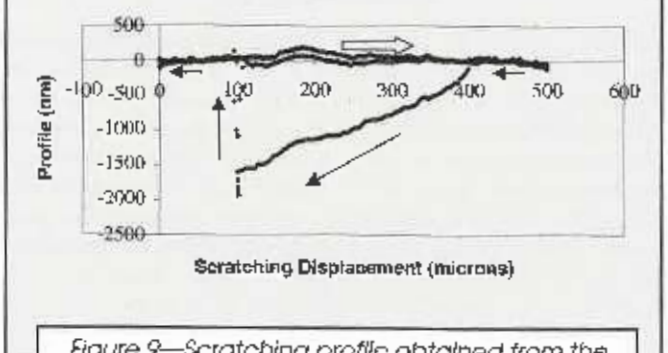

Figure 9—Scratching profile obtained from the surface of a pigmented coating produced with 11 min of baking. Arrows show direction of the scratch. The thicker arrow indicates the route that was followed twice.

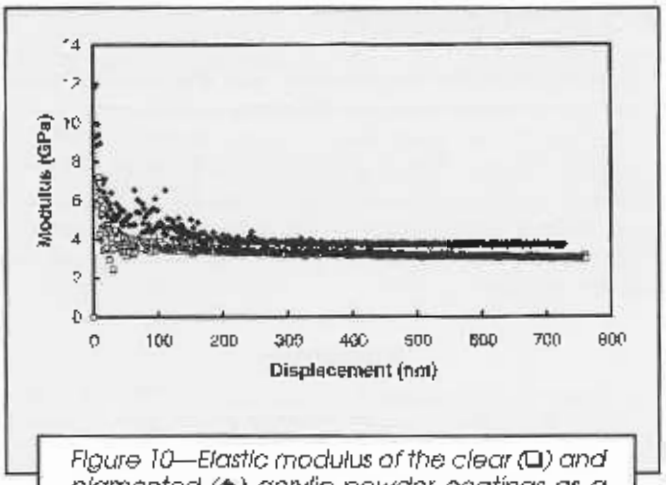

Figure 10—Elastic modulus of the clear (□) and pigmented (◆) acrylic powder coatings as a function depth into the surface.

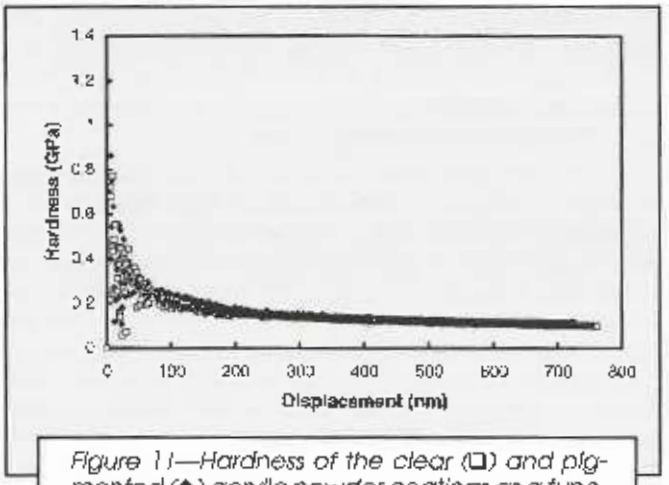

Figure 11—Hardness of the clear (□) and pigmented (◆) acrylic powder coatings as a function of indentation depth.

type are detected. That is, baking time does not affect the mechanical properties as reflected in the scratch profiles.

The post-scratch complete surface profiles are very similar to the initial profiles, thus indicating a nearly perfect elastic recovery after scratching for this level of deformation. Also, the roughness of the surfaces is found to remain within the initial, pre-scratch limits for all samples investigated. (Note that a perfectly elastic deformation would not leave a visible mar on the surface.) One would expect elastic behavior if the acrylic was fully-crosslinked at its surface so as to create an elastic network. By comparison, non-crosslinked acrylic surfaces[6] studied with nano-indentation show plastic deformation.

For the pigmented coatings, in the region of very low applied loads, the coefficient of friction was found to be ca. 0.35. A slightly higher value of ca. 0.4 was found for the linear region of the clearcoats.

Nano-Hardness

Figures 10 and 11 show the variation of the elastic modulus and hardness, respectively, as a function of indentation depth for both the clear and pigmented coatings after 11 min of baking time. These data are the result of averaging over six measurements. Both curves show a very steep decrease in the computed values at the beginning of indentation, which is attributed to the imperfections in the tip geometry.[7,5] Recent publications[6] emphasize that defects in the indenter tip might be of a size that is significant in comparison to the depth of indentation, and they might, therefore, cause significant errors in the hardness evaluation. To minimize such effects, special care was taken in using the same indentation geometry for all indentations. The tip geometry was calibrated against a fused silica substrate, as is described elsewhere.[6] Without due care, inaccuracies can arise in the tip calibration for penetration depths below 100 nm.

After the initial drop near the surface, constant values for the two mechanical constants are obtained. That is, there is no observed dependence of hardness or elastic modulus on depth into the coating. The average value of elastic modulus for the clearcoat (3 GPa) is slightly lower than for the pigmented coating (4 GPa). Both coatings approach an average nano-hardness value (plastic flow) of ca. 0.1 GPa. No significant differences in modulus or in hardness were found in samples having other baking times. For the range of times studied here, an increasing baking period (from 7 to 15 min) does not increase the coating surface hardness or stiffness. The implication of this finding is that the extent of crosslinking changes insignificantly after the first seven minutes of baking.

The values obtained here for the elastic modulus are very similar to those obtained elsewhere[11] from nano-indentation analysis of crosslinked acrylic coatings. Briscoe et al.[6] have reported a decrease in hardness and elastic modulus with increasing depth in glassy poly(methyl methacrylate) (PMMA) surfaces. In their data analysis, they specifically considered the effects of tip geometry, but they cannot rule out the effects of unestablished imperfections in the calibration procedure. At penetration depths greater than about 1000 nm, the elastic modulus of the PMMA approached 4 GPa, which is the value obtained here for a crosslinked acrylic. The hardness of PMMA was reported to approach about 0.25 GPa at depths beyond 1000 nm, which is likewise similar to values obtained here.

Courter[11] has reported previously that the modulus of crosslinked acrylics decreases with depth. An attempt was made to correlate the modulus depth dependence with a higher crosslink density at the surface. It is not clear if this work was also subject to the error induced by the effects of the tip geometry. Research using atomic force microscopy[10] has likewise concluded that the modulus of non-pigmented polyester and polyurethane coatings showed a depth dependence. Our finding of a uniform modulus with increasing depth differs from these other reports.

Scratching and nano-indentation analyses measure properties of materials' surfaces that are not expected to be the same as in the bulk. Nevertheless, for comparison to the data presented earlier, it is relevant to note that MEK double rub tests were performed on both the clearcoat and the pigmented coating. For both, there was no visual effect after 100 MEK double rubs. Macroscopic hardness tests were also performed. The Konig hardness

value obtained for the clearcoat formulation is 140 sec, whereas the pigmented coating has a value of 155 sec. Thus, there is an increase in the bulk hardness as a result of pigment addition, whereas there is no difference observed in the nanohardness values.

As shown previously in *Figure* 6, the clearcoatings surfaces displayed "micro-dimples." Experiments were performed with the aim of determining if these variations in topography could be correlated with mechanical properties. Indentation within the micro-dimples of the clearcoatings showed no significant differences in either the hardness or the elastic modulus of these regions in comparison to the smooth regions of the same samples. Thus, in summary, we see uniform mechanical characteristics at the sample surface—both laterally and with depth—and these characteristics are independent of the stoving time and only slightly sensitive to the presence of pigment.

CONCLUSIONS

Recently developed and improved techniques in thermal analysis, surface profiling, nano-scratching, and indentation were used to determine the properties of crosslinked acrylic powder coatings. Data regarding the effects of pigment addition on the curing, the visual appearance, and the near-surface mechanical properties were obtained. Several specific conclusions may be drawn.

Although the standard, as-recommended baking time for these acrylic formulations is 15 min, the nano-mechanical properties obtained after a baking time of seven minutes do not change significantly with additional baking times at the same temperature. The presence of the pigment increases the modulus of the coating surface slightly from 3 GPa to 4 GPa. Although the scratching experiments suggested that the pigmented coating has a slightly higher hardness than does the clearcoat, indentation experiments find no significant difference but an average value of 0.1 GPa in both. All of the coatings, regardless of their baking time or the presence of the pigment, showed extensive elastic recovery after the scratching and no significant extents of plastic deformation.

A decrease in elastic modulus was seen near the coating surface that is attributed to the effects of the stylus tip geometry. After this initial drop, the modulus remains constant. Thus, the data indicate that curing is complete at the surface, so that a fully elastic network is formed with a modulus that does not change significantly with penetration from the surface.

A smoother coating surface is achieved upon the addition of pigment to the acrylic. The non-pigment acrylic coating displays shallow "micro-dimples" (ca. 100 μm diameter) at its surface. The appearance of the film surface within these dimples does not differ from the rest of the coating. Moreover, the hardness and elastic modulus of the coating within these dimpled regions is identical, within experimental error, to the properties outside these regions. Thus, there is no evidence for non-uniformity in the amount of crosslinking laterally in the coating that can be correlated with the dimple formation.

ACKNOWLEDGEMENTS

We thank the UK Engineering and Physical Sciences Research Council and the Ministry of Defence/DERA (GR/L49277) for providing funding for DCA and this research. We also thank Dr. Jim Janimak at the Polymer Research Centre, University of Surrey, for technical support in the MTDSC analyses. Furthermore, we acknowledge the support of Veeco, Cambridge in obtaining the surface profiles.

References

(1) Busato, E., "Waterborne & Powder Coatings 1998-2010. Is Past Growth Sustainable?," *Fifth Nurnberg Congress Papers*, 2, 5 (1999).
(2) De Lange, P.G., "Film Formation and Rheology of Powder Coatings," JOURNAL OF COATINGS TECHNOLOGY, *56*, No. 717, 23 (1984).
(3) Kenny, J.C., Ueno, T., and Tsutsui, K., "Analytical Approach for High Quality Appearance Powder Coatings," JOURNAL OF COATINGS TECHNOLOGY, *68*, No. 855, 35 (1996).
(4) Schallamach, A., "Abrasion of Rubber by a Needle," *J. Polym. Sci.*, 9, 385 (1952).
(5) Briscoe, B.J., Evans P.D., and Lancaster, J.K., "Single Point Deformation and Abrasion of γ-Irradiated Poly(tetrafluoroethylene)," *J. Phys. D: Appl. Phys.*, 20, 436 (1987).
(6) Briscoe, B.J., Fiori, L., and Pelillo, E., "Nano Indentation of Polymeric Surfaces," *J. Phys. D: Appl. Phys.*, 31, 2395 (1998).
(7) Briscoe, B.J., Pelillo, E., Ragazzi, F., and Sinha, S.K., "Scratch Deformation of Methanol Plasticised Poly(methylmethacrylate) Surfaces," *Polymer*, 39, No. 11, 2161 (1998).
(8) Phair, R.J., "Testing Techniques and Uses of Equipment for Evaluating Organic Coatings," *Paint and Varnish Production*, 30, No. 7, 12 (1950).
(9) Briscoe, B.J., Pelillo, E., and Sinha, S.K., "Scratch Hardness and Deformation Maps for Polycarbonate and Polyethylene," *Polym. Eng. Sci.*, 36, No. 24, 2996 (1996).
(10) Shen, W., Stanley, M.S., Jones, F.N., Caigui, L., Ryntz, R.A., and Everson, M.P., "Use of a Scanning Probe Microscope to Measure Marring Mechanisms and Micro-Hardness of Crosslinked Coatings," JOURNAL OF COATINGS TECHNOLOGY, 69, No. 873, 123 (1997).
(11) Courter, J.L., "Micro-and Nano-Indentation and Scratching for Evaluating the Mar Resistance of Automative Clearcoats," *Fifth Nurnberg Congress*, 1, 353 (1999).
(12) Courter, J.L., "Mar Resistance of Automative Clearcoats: I. Relationship to Coating Mechanical Properties," JOURNAL OF COATINGS TECHNOLOGY, 69, No. 866, 57 (1997).
(13) Lin, L., Blackman, G.S., and Matheson, R.R., "Micro-Mechanical Characterization of Mar Behaviour of Automotive Topcoats: Micro- and Nano-Wear of Polymeric Materials," *Abstracts of Papers*, Am. Chem. Soc., 216(3), 593-POLY (1998).
(14) Blackman, G.S., Lin, L., and Matheson, R.R., "Micro and Nano-Wear of Polymeric Materials," *Abstracts of Papers*, Am. Chem. Soc., 216(3), 591-POLY (1998).
(15) Reading, M., Elliot, D., and Hill, V., "A New Approach to the Calorimetric Investigation of Physical and Chemical Transitions," *J. Therm. Anal.*, 40, 949 (1993).
(16) Reading, M., "Modulated Differential Scanning Calorimetry—A New Way Forward in Materials Characterisation," *Trends in Polym. Sci.*, 8, 248 (1993).
(17) Bohn, K.P., Prahm, A., Petersson, J., and Kruger, J.K., "Modulated Differential Scanning Calorimetry: Investigation at Structural Phase Transitions," *Thermochim. Acta*, 305, 283 (1997).
(18) Hourston, D.J., Song, M., Hammiche, A., Pollock, H., and Reading, M., "Modulated Differential Scanning Calorimetry. 6. Thermal Characterization of Multicomponent Polymers and Interfaces," *Polymer*, 38, No. 1, 1 (1997).
(19) Androsch, R., "Melting and Crystallization of Poly(ethylene-co-octane) Measured by Modulated DSC and Temperature-Resolved X-ray Diffraction," *Polymer*, 40, No. 10, 2805 (1999).
(20) Reading, M., Luget, A., and Wilson, R., "Modulated Differential Scanning Calorimetry," *Thermochim. Acta*, 238, 295 (1994).
(21) Wunderlich, B., Jin, Y., and Boller, A., "Mathematical Description of Differential Scanning Calorimetry Based on Periodic Temperature Modulation," *Thermochim. Acta*, 238, 277 (1994).

(22) Misev, T.A., *Powder Coatings: Chemistry and Technology*, John Wiley and Sons, Chichester, 1991.
(23) Thames, S.F., Panjnani, K.G., Pace, S.D., Blanton, M.D., and Cumberland, B.R., "Novel Organosilane Crosslinking Agents for Powder Coatings," JOURNAL OF COATINGS TECHNOLOGY, 67, No. 841, 39 (1995).
(24) Van Mele, Bruno, Van Assche, G., Hemelrick, A., and Rahier, H., "Modulated DSC™ Evaluation of Isothermal Cure and Vitrification for Thermosetting Systems," *Thermochim. Acta*, 268, 121 (1995).
(25) Doerner, M.F. and Nix, W.D., "A Method for Interpreting the Data from Depth-Sensing Indentation Instruments," *J. Mater. Res.*, 4, 601 (1986).
(26) Oliver, W.C. and Pharr, G.M., "An Improved Technique for Determining Hardness and Plastic Modulus Using Load and Displacement Sensing Indentation Experiments," *J. Mater. Res.*, 7, No. 6, 1664 (1992).
(27) Yeates, S.G., Annable, T., Denton, B.J., Ellis, G.M., Nasir, R.M.D., Perito, D., and Parker, I., "Rheology of Acrylic Powder Coatings," JOURNAL OF COATINGS TECHNOLOGY, 68, No. 861, 107 (1996).
(28) Orchard, S.E., "On Surface Levelling in Viscous Liquids and Gels," *Appl. Sci. Res. A*, 11, 451 (1962).
(29) Andrei, D.C., Hay, J.N., Keddie, J.L., Scar, R.P., and Yeates, S.G., "Surface Levelling of Thermosetting Powder Coatings: Theory and Experiment," *J. Phys. D: Appl. Phys.*, 33, 1975 (2000).